Evidence for a size-dependent transition between noncrystalline structures and crystalline structures with defects in frozen Lennard-Jones clusters

W. Polak

Department of Applied Physics, Institute of Physics, Lublin University of Technology, ul. Nadbystrzycka 38, 20-618 Lublin, Poland

(Received 4 January 2007; revised manuscript received 19 October 2007; published 18 March 2008)

Liquid Lennard-Jones clusters of 14 different sizes from $N=55-923$ atoms were cooled down in Monte Carlo simulations (40 runs for each size) to the reduced temperature $T^*=0.05$. Structural analysis and visualization were applied for classification of the internal structure of all 560 final clusters. Small clusters revealed the presence of the multishell icosahedra or regular polyicosahedra. In larger clusters, beginning from $N=309$, the noncrystalline atom ordering is often replaced by the formation of defected crystalline clusters in the form of layered face-centered cubic–hexagonal close-packed (fcc-hcp) clusters or defected layered clusters with some additional nonparallel hcp overlayers. The presence of regular polyicosahedral clusters, relatively numerous even at the largest analyzed sizes, is attributed to kinetic effects in structure formation.

DOI: 10.1103/PhysRevE.77.031404 PACS number(s): 61.72.Nn, 36.40.−c, 02.70.Uu, 82.20.Wt

I. INTRODUCTION

It is commonly accepted that cluster structure is size dependent. In the case of rare-gas atoms, investigation of transition size from noncrystalline icosahedral (ic) or decahedral (dh) to crystalline face-centered cubic (fcc) or hexagonal close-packed (hcp) structures gives very different results. Experiments with argon cluster beams revealed transition sizes with the number of atoms: $N=750$ in the cluster as given by Farges *et al.* [1], from $N=1500-3500$ as reported by Lee and Stein [2], $N=1500$ as established by Kovalenko *et al.* [3], and finally, $N=200$ as observed by Kakar *et al.* [4] for the first occurrence of fcc structure.

The above experimental data do not agree with the theoretical results obtained by comparing the potential energy of different cluster structure, which gives much greater transition sizes. For example, using the Lennard-Jones (LJ) potential for interatomic interactions, Raoult *et al.* [5] predicted the formation of fcc crystalline clusters at $N=100\,000$, while Doye and Calvo [6] reported a value of $N=213\,000$. It is worth mentioning that very recently, Krainyukova [7] excluded transition to the fcc structure at very large LJ cluster sizes and predicted that the hcp clusters are the most favorable above $N\approx 34\,000$.

The discrepancy between the theory and the experiment can be caused partly by serious difficulty in the determination of cluster structure in experiments [8], and partly by the weakness of theoretical considerations based on searching a global minimum of cluster potential energy at temperature $T=0$. Baletto and Ferrando [9] argued that a satisfactory explanation of experimental outcome (here, cluster structure) is often impossible from energetic considerations alone because it is formed as a result of complex dynamical interplay between energetic, thermodynamic, and kinetic effects involved during cluster formation. Computer simulations are the unique way to include all these effects into analysis.

The first important simulation results on structural transition in LJ clusters were reported by Ghazali and Lévy [10], who analyzed a wide class of LJ interactions. For the classical LJ 6–12 potential, they reported a transition from icosahedral to defected crystalline clusters at $N\approx 300$, a size very small in comparison with the sizes predicted from minimum of cluster potential energy. The second important step towards understanding size-dependent structure transition was taken by Ikeshoji *et al.* [11], who realized the LJ cluster solidification using molecular dynamics simulations. They observed gradual transition from icosahedral to decahedral, fcc, and hcp (sparse) internal structures around $N=450\pm 100$. The presence of defects (twins and stacking faults) in most of the fcc clusters was easily detected.

The two above-mentioned papers [10,11] are not precise in their description of the cluster internal structure because the authors used plane projections of cluster atoms. This kind of visualization produces pictures with evident symmetry in atomic arrangement when the cluster structure is nearly perfect, but the picture is unclear in the case of defected clusters which are dominant at larger sizes [10,11]. The second weakness is the limitation of computations to one run for a given N. This hinders theoretical analysis because size-dependent effects are covered by stochastic effects in cluster-structure formation observed for a constant N.

This paper is focused on the precise analysis of the internal structure of frozen LJ clusters in order to prove the possibility of the structural transition and confront the results with the existing theoretical and experimental data. Therefore, the simulations were planned to form many (here 40) cold clusters for 14 given sizes: $N=55$, 62, 75, 81, 110, 147, 201, 222, 309, 450, 561, 700, 810 and 923, selected in the region of expected structural transition. For each size, 21 final clusters were taken directly from the previous simulated data, analyzed and described recently [12] solely in the context of size dependence of freezing temperature and structural fluctuations near freezing region. In order to improve the statistics of cluster structure, 19 additional simulations were realized for every size.

The internal structure of all 560 final clusters, sufficiently cold to have good ordered and stable structure, was analyzed using the newly developed coordination polyhedron method [13] followed by the visualization of cluster structure, which also enables one to classify defected clusters. The emphasis in this work is not on the method of cluster formation, which is presented in Ref. [12], but is on: (i) comprehensive pre-

sentation of all types (several are quite new) of internal structure of frozen LJ clusters, (ii) convincing observation of the size dependence of cluster structure, and (iii) observation of the kinetic effect in the formation of some cluster structures.

II. SIMULATION METHOD

Cluster production in the adiabatic expansions of a rare gas leads to the formation of beams of liquid clusters [14], which subsequently cool down by atom evaporation and thermal radiation attaining a sufficiently low temperature to be solidified. Such a process of cluster formation is very difficult to mimic in computer simulations. For example, even simplified simulations of cluster formation process during cooling a source gas (represented by 65 536 atoms in the simulation cell) in supersonic beams, as presented by Ikeshoji *et al.* [15], lead to many small maximal clusters of $N<250$. In order to form and analyze one solid cluster of a given size it is better to freeze a liquid cluster (nanodroplet) in computer simulations. This method is valid for solidification occurring after cessation of a cluster growth but induced by decreasing cluster temperature caused by surrounding cold inert gas. Ikeshoji *et al.* [11] carried out freezing in molecular dynamics simulations by enabling cluster evaporation and thermostatic cooling. In the present work, the cooling of liquid cluster is achieved using Monte Carlo (MC) simulations. The main assumptions of the model and the cooling method, used in the simulations, are given below, but detailed description and all simulation parameters can also be found in the author's recent work [12].

The cooled cluster is placed in the center of the cubic simulation box repeated periodically in the three-dimensional space. These periodic boundary conditions not only enable evaporation of some atoms into cluster surroundings in the box when the cluster is hot, but also enable catching all vapor atoms by the sufficiently cooled cluster. The system or cluster temperature T is decreased in a steplike manner, i.e., after each instant temperature decrement ΔT, the temperature is kept constant for a certain simulation time. The remaining two system parameters, the volume V of the simulation box and the number N_s of atoms in the system, are always constant. It means that at a given simulation stage when T is constant, the canonical Monte Carlo method has been implemented.

At all simulation stages, each LJ atom in the system tries many times to change its position to adopt system parameters, for example, the cluster structure, to the actual temperature. The probability for position change of an ith atom is strictly connected with the value of the interaction energy U_i of the atom with all remaining atoms in the system. The atoms are assumed to interact by the classical Lennard-Jones 6–12 potential as follows:

$$U(r_{ij}) = 4\varepsilon\left[\left(\frac{\sigma}{r_{ij}}\right)^{12} - \left(\frac{\sigma}{r_{ij}}\right)^{6}\right], \tag{1}$$

where r_{ij} is the interatomic distance while σ and ε are the values of the potential parameters which are known in the literature for different rare gases. Because the LJ interaction is very small at larger distances, their value is neglected for interatomic distance larger than the truncation distance $r_{tr}=3.4\sigma$. This significantly speeds up computations of interaction energy U_i necessary for accepting or rejecting the position change or jump of the ith atom. The acceptance probability p for the proposed jump is given by the Metropolis criterion in the form

$$p = \exp(-\Delta U_i/k_B T), \tag{2}$$

where $\Delta U_i>0$ denotes an increase in the interaction energy due to the ith atom jump and k_B is the Boltzmann constant. All jumps are accepted if they lead to a decrease in the interaction energy, i.e., $p=1$ if $\Delta U_i<0$. In one MC cycle, there were N_s attempts to displace randomly selected atoms in the system.

The length of a simulation stage, expressed in the number of MC cycles realized during the run, must be large enough to enable good thermalization of the cluster and related to the value of cluster temperature change. When a cluster transition from liquid to solid state or fluctuations between these states were expected [12], the system temperature was changed slowly, i.e., after each 200 000 MC cycles by $\Delta T=0.01k_B/\varepsilon$ ($\Delta T^*=0.01$ when the temperature is expressed in reduced units k_B/ε). This enables sufficient thermalization of a forming solid cluster structure and does not allow trapping in a highly metastable state, for example, in a glassy state from rapidly cooled liquidlike cluster. Below this region, i.e., after the stable cluster freezing, the structural changes are minimal. Therefore, the much larger temperature change $\Delta T^*=0.05$ was applied after each 400 000 MC cycles in order to reach the final temperature $T_f^*=0.05$ (equivalent to 6 K for argon) during a shorter simulation time.

The cluster cooling simulations were realized to obtain 40 solid LJ clusters at the final temperature T_f for each cluster size N. While 21 final clusters were taken directly from the existing simulation data [12], the remaining 19 clusters were obtained in additional simulation runs realized in an identical way. For a given N, every simulation was started from the same liquid cluster but with a different seed in the random number generator, which is sufficient to produce a unique arrangement of cluster atoms during cooling.

This paper is limited to a detailed analysis of the internal structure of all final clusters. The fast and precise detection of cluster structural units, each understood as a central atom and 12 regularly located first neighbors, was enabled by the coordination polyhedron method [13] using the sphere radius in the range $1.15\sigma \leqslant R_n \leqslant 1.40\sigma$ to embrace all the first neighbors and the radius increment $\Delta R_n=0.01\sigma$. The spatial location of structural units is best visible in four graphic images of the cluster, each presenting central atoms of detected units, separately for fcc, hcp, ic, and dh structures. Two central atoms of the same structural type are linked if they are neighbors. Moreover, to indicate better positions of ic units, which are often sparse and separated, every central atom is enclosed in icosahedron built by linking its neighbors. When all cluster images were carefully analyzed, it was ascertained that most of the obtained clusters show a regular atom arrangement and can be grouped into seven types, which are discussed in detail below.

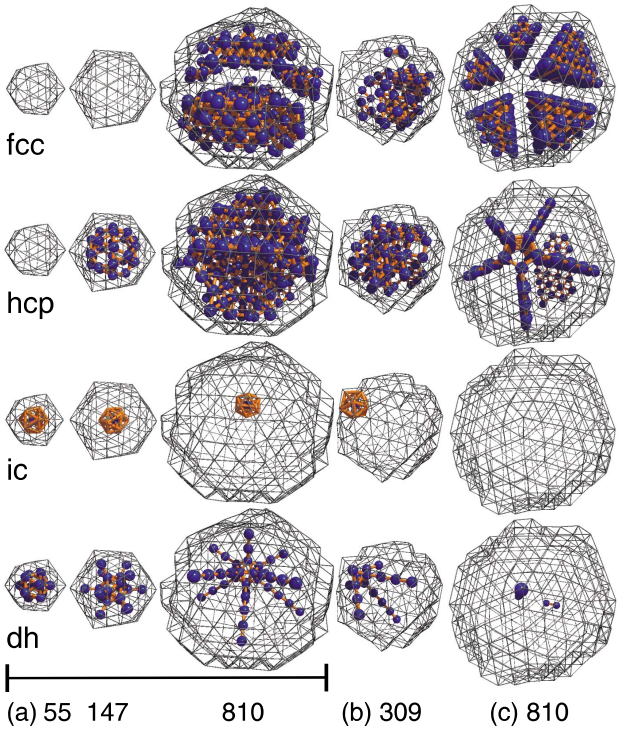

FIG. 1. (Color online) Icosahedral clusters with their point of symmetry located near (a) cluster center (MIC type) or (b) cluster surface (s-IC type). (c) Decahedral atom ordering with the dh chain along the line of fivefold symmetry.

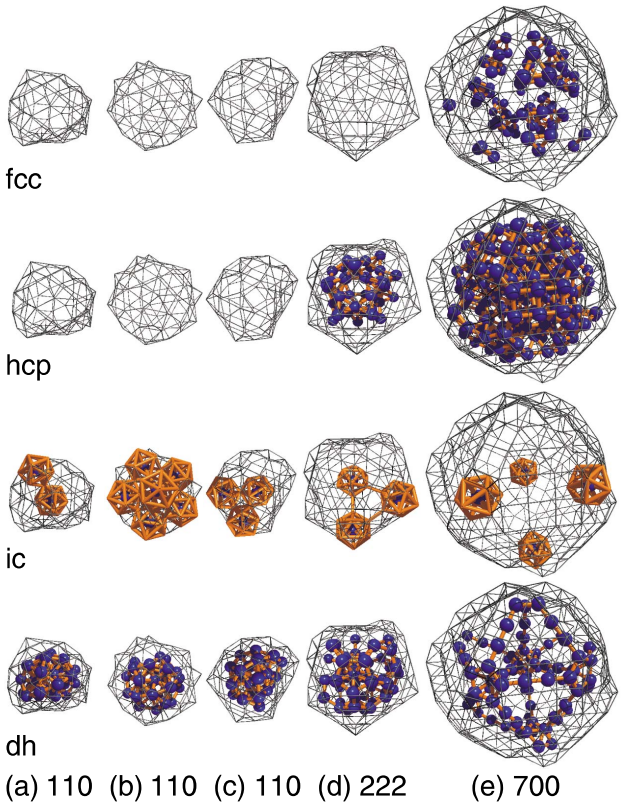

FIG. 2. (Color online) Regular polyicosahedral clusters characterized by the presence of several regularly located ic units, many dh units, and (in sufficiently large clusters) hcp and fcc units.

III. INTERNAL STRUCTURE OF SOLID CLUSTERS

A. Noncrystalline clusters with one center or line of fivefold symmetry

Clusters revealing a structure similar to that of the Mackay clusters are included in the group of noncrystalline clusters with global fivefold symmetry in atom arrangement [Fig. 1(a)]. They are multishell icosahedral clusters (MIC) characterized by one center of icosahedral symmetry reaching the entire cluster with or without regular external shape, and six linear chains of local decahedral units crossing near the cluster center. The subgroup of MIC clusters is Mackay clusters, which possess 20 flat triangular dense-packed {111} faces forming ideal icosahedron. When the center of an icosahedral structure is located on the cluster surface and is connected with several dh chains passing in different directions through the cluster [see Fig. 1(b)], the cluster is called surface-centered icosahedral (s-IC). In this work, the formation of these quite new s-IC clusters is reported to occur frequently, often during the freezing of the liquid LJ clusters.

Another type of global fivefold symmetry is found in well-known decahedral clusters characterized by the fivefold symmetry around the linear chain of dh units coming near the cluster center accompanied by five hcp planes crossing themselves and five fcc sectors [Fig. 1(c)]. The dh clusters observed here always possess some additional hcp surface planes as a result of stacking faults on the dense-packed {111} surfaces. Those hcp surface monolayers, which cross one of the existing five hcp monolayers at an acute angle close to 70.5° [16], are preferred in formation. At this cross line, an additional dh chain is typically formed. The cluster visible in Fig. 1(c) has the main dh chain composed of 8 dh units and the additional short chain of 2 dh units formed by 2 hcp surface planes.

B. Noncrystalline clusters with regular polyicosahedral structure

A large part of the clusters belongs to the new group of regular polyicosahedral (r-PIC) clusters whose characteristic feature is the presence of several (from two up to even seven) ic units, which are regularly located inside the cluster, as presented in Fig. 2. Inherently present in the investigated cluster size are also some dh units, while hcp and fcc units appear at a sufficient cluster size. Polyicosahedral (PIC) clusters were observed [17] nearly 20 years ago in experimental and simulated argon clusters with less than 50 atoms, where icosahedral units interpenetrate or contact themselves by sharing one triangular face. Regularity in the structure of polyicosahedral clusters was observed quite recently [13] when analyzing LJ clusters with $N=201$. Now, it can be said that, for all analyzed cluster sizes $62 \leqslant N \leqslant 923$, the r-PIC structure is commonly found. As shown in Fig. 2, the icosahedral units are regularly positioned one against another; they usually form pair, regular triangle, or regular tetrahedron. When the number of icosahedral units exceeds four,

their spatial arrangement also reveals the existence of a few regular triangles or tetrahedrons.

Detailed observations of the clusters analyzed here revealed that icosahedral units are located mostly at the cluster surface as shown in Fig. 2. In the case of small clusters, icosahedral units always contact themselves with vertices. With increasing N, the cluster diameter increases. Therefore, already at $N=201$, some ic units do not contact but are linked with a cylinder of length equal to the first neighbor distance [Fig. 2(d)]. As the cluster size increases further, beginning from $N=309$ the local ic units lose links due to increased separation distance [Fig. 2(e)].

For larger clusters ($N \geqslant 450$), the internal symmetry can be detected better by observation of chains formed by decahedral units [Fig. 2(e)]. In such large r-PIC clusters, decahedral chains constitute edges of regular triangles or tetrahedrons, while icosahedral units are located at cross points. Inside a sufficiently large regular tetrahedron, limited by decahedral lines, an fcc domain of tetrahedral shape also exists. Nice examples of r-PIC structure, characterized by long and numerous (e.g., 12) dh chains, were observed earlier in the case of growing LJ clusters, but they were called polytetrahedral [16]. One of them is shown in the paper [16] for $N=1650$ as the typical internal structure formed at the growth temperature $T^*=0.35$.

C. Defective crystalline clusters

There are clusters where no ic unit is present, but the structure is created by crystalline fcc and hcp units forming dense-packed {111} layers. Since no cluster composed exclusively of fcc or hcp structure was found, they are called defected crystalline. Three types of such clusters are observed: layered fcc-hcp, defected layered fcc-hcp and tetrahedral fcc. These types of structures can be detected very easily by observing the spatial position of hcp local structure or that of dh chains.

The layered fcc-hcp clusters [Fig. 3(a)] are characterized by the presence of some parallel fcc and hcp layers put alternatively one above another. The formation of new parallel layers was attributed [16] to the misposition of atoms added to the growing cluster leading there to parallel stacking faults. In the case of cluster solidification analyzed here, the misposition must occur during the growth of a solid fcc or hcp nucleus inside a liquid supercooled cluster.

Sufficiently large frozen clusters also revealed that hcp surface defects in layered fcc-hcp clusters, with one [Fig. 3(b)] or two [Fig. 3(c)] additional nonparallel hcp layer(s) at the acute angle close to 70.5° [16] with respect to the direction of fcc-hcp boundary, are a general feature. Clusters with four nonparallel hcp layers, which represent all different directions of dense-packed {111} planes in the fcc structure [18], surrounding the fcc region of tetrahedral shape are often observed. Their detection is easier when one observes the form of fcc domains. As shown in Fig. 3(d), apart from the dominating tetrahedral fcc core usually located near the cluster center, some fcc layers parallel to tetrahedron planes may also exist. The hcp layers lying on the fcc core form more or less a complete tetrahedron cage. In tetrahedral fcc clusters some (maximum six) linear chains of decahedral units, which are parts of tetrahedron edges, are also present.

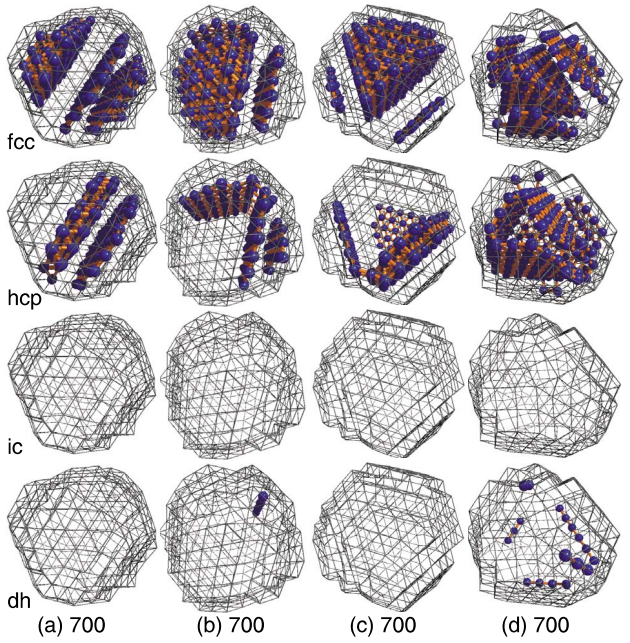

FIG. 3. (Color online) Defective crystalline clusters: (a) layered fcc-hcp, [(b) and (c)] defected layered fcc-hcp, and (d) tetrahedral fcc.

IV. STATISTICS AND ENERGY OF CLUSTER STRUCTURES

The detailed statistics of cluster structures shown in Fig. 4 reveals a significant dependence of the number of different cluster types on size N. Below $N=309$, the multishell icosahedral or regular polyicosahedral atom ordering dominates in the cluster spectrum. The MIC clusters are usually formed at the magic numbers $N=55$ and 147 or close to them as in the

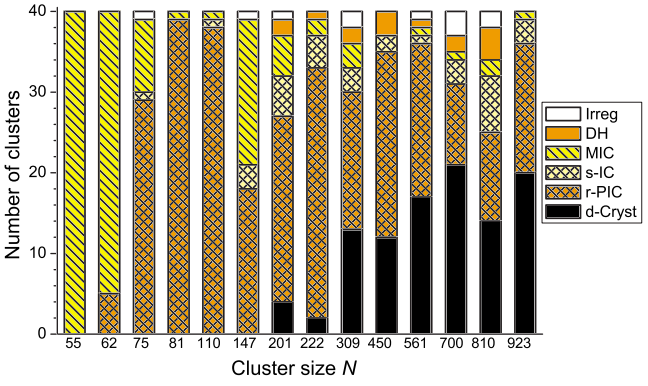

FIG. 4. (Color online) Histograms of different types of structures among 40 clusters obtained for each analyzed size. Abbreviations in the legend: Irreg (irregular), dh (decahedral), MIC (multishell icosahedral), s-IC (surface-centered icosahedral), r-PIC (regular polyicosahedral), and d-Cryst (defective crystalline) cluster.

TABLE I. Sequence of the three lowest potential energy per atom $E_p(N)/N$ of clusters cooled down to $T^*=0.001$ compared with the global minima. Abbreviations used for cluster structure description are L, layered fcc-hcp; dL, defected layered fcc-hcp; t-fcc, tetrahedral fcc; MIC, multishell icosahedron; s-IC, surface-centered icosahedron; r-PIC, regular polyicosahedral; and dh, decahedral. Last column shows the energy difference between first and global minimum.

N	Global minimum	First minimum	Second minimum	Third minimum	$\Delta E_p/E_p$
110	MIC: −5.652620 [19,20]	MIC: −5.6400	r-PIC: −5.5981	r-PIC: −5.5980	0.22%
147	MIC: −5.962321 [19,20]	MIC: −5.9606	MIC: −5.9434	MIC: −5.9433	0.03%
201	MIC: −6.149872 [21]	r-PIC: −6.1270	MIC: −6.1265	MIC: −6.1238	0.37%
222	MIC: −6.228337 [21]	MIC: −6.2193	MIC: −6.2168	s-IC: −6.1938	0.15%
309	MIC: −6.495854 [21]	dh: −6.4265	MIC: −6.4209	MIC: −6.4147	1.07%
450	MIC: −6.700365 [19]	L: −6.6597	t-fcc: −6.6583	L: −6.6570	0.61%
561	MIC: −6.849186 [19,22]	s-IC: −6.7952	r-PIC: −6.7878	MIC: −6.7852	0.79%
700	MIC:[a] −6.951257 [19]	t-fcc: −6.9192	s-IC: −6.9137	t-fcc: −6.9115	0.46%
810	MIC:[a] −7.024596 [19]	t-fcc: −6.9935	s-IC: −6.9929	dL: −6.9912	0.44%
923	MIC: −7.099374 [19,22]	L: −7.0531	L: −7.0516	s-IC: −7.0507	0.65%

[a]Multishell icosahedron with the central vacancy [23].

case of $N=62$. In the case of $N=55$, all simulated clusters attain the MIC form corresponding to the Mackay icosahedron. For $N=147$, the number of MIC clusters is much smaller (18 per 40 with only several Mackay clusters) but is strikingly high when compared with the neighbors: one MIC at $N=110$ and five at $N=201$. Larger clusters with $N\geqslant 222$ relatively seldom attain the MIC structure: one or two cases were registered for each size (three for $N=309$), while none were registered for $N=450$.

The main competitors for MIC clusters, frequently found in the spectrum of smaller clusters with $N<200$, are the r-PIC clusters. The regular PIC clusters dominate the spectrum when N is far from the magic numbers 55 and 147. However, in contrast to MIC clusters, the regular polyicosahedral clusters are present in a significant amount up to the largest size $N=923$. In the range of $201\leqslant N\leqslant 561$, the r-PIC structure prevails.

Beginning from $N=309$, the r-PIC clusters are often replaced by defective crystalline clusters. The percentage of such a cluster type in this size range remains at a relatively high level between 30 and 50 %. It should be noted that the first four defective crystalline clusters with the presence of the fcc structure were obtained already at $N=201$ in accordance with experimental results of Kakar *et al.* [4].

Changes in the abundance of different types of cluster structures should be correlated with the value of the cluster potential energy E_p, if structure formation is governed by energetic effects. The potential energy per atom E_p/N and its standard deviation were calculated separately for all structural types of final clusters at $T^*=0.05$ using the LJ potential [Eq. (1)] without any cut off, which means that all pairs of cluster atoms contribute to the cluster potential energy. This value, free of the cutting-off errors, was used to find the best bonded final clusters at a given N. Minimum three clusters of the lowest potential energy $E_p(N)$, i.e., with the highest bonding energy, were cooled down in additional simulations to attain the temperature close to zero, i.e., $T^*=0.001$. Their final potential energy is compared in Table I with the global minima known from the database [19].

The results from Table I show that all clusters analyzed in this work are bonded slightly weaker than the corresponding global minimum from the literature. The energy difference can be explained mainly by a nonoptimal cluster structure as, for example, in the case of the regular PIC clusters of $N=201$ from Table I. However, some part of this energy difference can be eliminated if atomic positions are determined precisely at the absolute temperature (cf. the value for the first and global minimum at $N=147$ for the same Mackay cluster) or positions of surface atoms are optimized to avoid isolated atoms or small islands.

Although the defected clusters found here do not have the lowest potential energy, the difference is only ca. 0.6% (see Table I) with respect to the value of global minimum when largest sizes with $N\geqslant 450$ are concerned. These clusters are significantly better bonded than the octahedral fcc clusters with $N<1000$ and have an energy comparable with the hcp clusters of the same size, as may be deduced from the plot in the recent report of Krainyukova [7]. Therefore, all new cluster structures from Table I (surface-centered icosahedral, regular polyicosahedral, tetrahedral fcc, layered fcc-hcp or defected layered fcc-hcp) should be considered as candidates for the structure of frozen liquid rare-gas clusters.

Two cluster structures, regular polyicosahedral and defected crystalline, most frequently found at larger sizes, were precisely analyzed regarding their average bonding energy. Surprisingly, all defected crystalline clusters turned out to be more strongly bonded than r-PIC clusters of the same size $N\geqslant 309$ or their energy is only very slight smaller for $N=201$ and 222 (Fig. 5). When E_p/N is plotted against $N^{-1/3}$ (Fig. 5) for $201\leqslant N\leqslant 923$ the data points lie, in the range of the standard deviation, on two straight lines, each expressed by

$$E_p/N = a + bN^{-1/3}, \tag{3}$$

where a and b are empirical constants. The location of the points on the best-fit line is exceptionally good for all de-

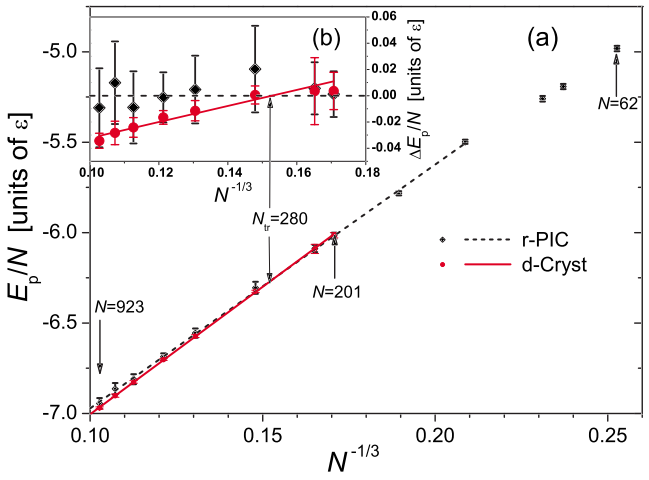

FIG. 5. (Color online) (a) Average potential energy per atom, its standard deviation and approximating line for two types of LJ clusters: regular polyicosahedral (r-PIC) and defected crystalline (d-Cryst). (b) Difference between the cluster energy and the approximated energy value for r-PIC and defected crystalline clusters of the size $N \geqslant 201$. The crossing of the two approximating lines at $N_{tr}=280$ lines is interpreted as the predicted transition size between the r-PIC and d-Cryst cluster structures.

fected crystalline and satisfactory for r-PIC clusters with $N \geqslant 110$, although for lower $N=81$, 75, and 62 some deviation from linearity may be observed. The parameters a and b derived from the weighted least-square method are the following: −8.3198 and 13.482 for r-PIC, while −8.4131 and 14.093 for defected crystalline clusters. The lines cross each other at $N=280$ [see Figs. 5(a) and 5(b)], which can be regarded as the transition size from noncrystalline r-PIC to defected crystalline structures, as predicted from energetic considerations.

V. KINETIC EFFECTS IN STRUCTURE FORMATION

The fact that r-PIC clusters for $N=309$, 450, and 561 are the most abundant may reflect insufficient cluster statistics obtained from 40 simulation runs. However, there are observations of cluster structure formation convincing one that it is a result of kinetic effects during freezing. Unstable icosahedral units located preferably near the surface of supercooled cluster [24] are able to induce solidification to the r-PIC or s-IC structures, which are characterized, respectively, by several ic units and one ic unit present on the surface.

The mechanism is very well illustrated by the cluster structure evolution in Fig. 6. The cluster shown in Fig. 6(a) with two icosahedral units and one unit representing each solidlike structure fcc, hcp, and dh is classified as liquid [12] or better as supercooled liquid. Then, the formation of a small solid nucleus composed of several fcc, hcp, and dh units is observed in Fig. 6(b) inside the cluster in the presence of temporary icosahedral units on the surface. The formed nucleus changes often its atomic arrangement and significantly its position but remains. The stability of the nucleus structure is more firm when the structure is attached to an ic unit [Fig. 6(c)] composed of 13 atoms (12 neighbors and one ic center) on the cluster surface.

The icosahedral unit induces characteristic atomic arrangement into the solidifying cluster because dh linear

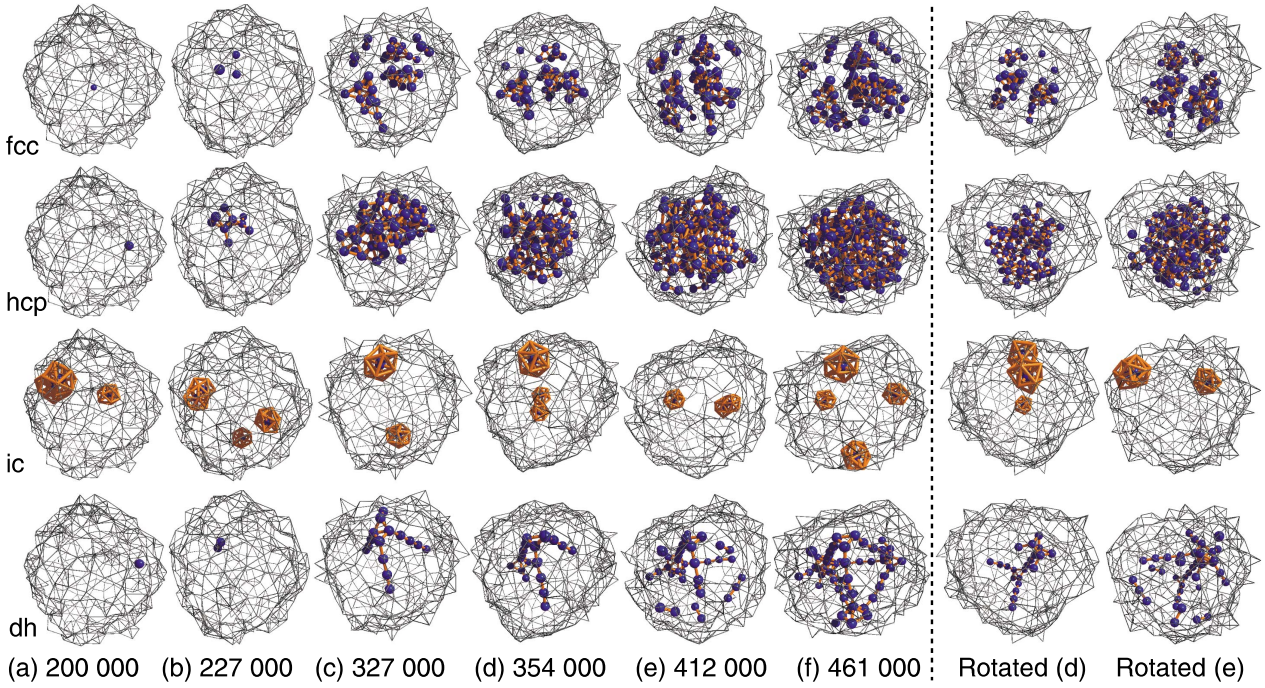

FIG. 6. (Color online) [(a)–(f)] Structural evolution of a LJ_{810} cluster from a liquid to solid state of r-PIC character when initiated by a surface ic unit. Numbers of MC cycles from the beginning of this equilibration stage at $T^*=0.44$ are shown below the cluster pictures. Two rotated clusters illustrate more precisely the formation of a new surface ic unit possible when a dh linear chain reaches the cluster surface.

chains must be connected radially to vertices of the ic unit as can be deduced from positions of fivefold axes in ideal MIC clusters [13]. Therefore, decahedral linear chains [usually three or four as visible in Fig. 6(c)] elongate in different directions, but at the angle close to 60° with respect to one another. When they meet some other part of the surface, they typically initiate the formation of the next ic units [see Fig. 6(d)], where new dh chains are formed [Fig. 6(e)]. Since the initial and new-formed ic units on the ends of every dh chain are not twisted with respect to one another (fivefold symmetry is conserved along the chain), the directions of newly formed dh chains are precisely determined. As a result of such structure formation mechanism, the dh lines always meet themselves and form ideal triangles or tetrahedrons as in Fig. 6(f).

The proposed mechanism can explain structure formation in s-IC clusters [see Fig. 1], where the dh chains propagate inside a cluster during freezing but without successful formation of a next ic surface unit. Maybe this is because the cluster structure in the near-surface layer is very weak and often disappears since it is subjected to large atom movements. Consequently, some icosahedral units may vanish even if connected with the existing r-PIC structure inside the cluster [see the lack of the ic unit in the top part of the cluster in Fig. 6(e)]. Therefore, sometimes it can be found that some surface ic units in the final r-PIC clusters are absent although the internal structure is well arranged and easily detected from the regular network of dh chains.

Some other effect, not recognized yet, may also be responsible for the observed preference of defected crystalline clusters with respect to the small population of MIC and dh clusters for $N \geqslant 222$ (Fig. 4). From energetic consideration, these types of clusters should be nearly equal in number since all of them have a similar value of the potential energy.

VI. DISCUSSION AND CONCLUSIONS

Natural candidates for the comparison of cluster structure are large LJ clusters [11] solidified by cooling in the size range of $N=160$ up to 2200. Structures shown in Ref. [11] as fairly perfect decahedral or fcc clusters exhibit some of the imperfections resembling the hcp surface layers in dh and defected layered fcc-hcp clusters probably with a fcc layer dominating the cluster. Most of the solid structures formed by growth initiated from solid LJ_{201} and continued up to $N \approx 2000$ are identical with the defective crystalline (among them tetrahedral fcc, layered fcc-hcp, and defected layered fcc-hcp), decahedral, and r-PIC clusters [16].

Noya and Doye [25] reported that the internal structures formed during solid-solid transformations in LJ_{309} are aggregates of fcc tetrahedra. It seemed that two or three of them are regular polyicosahedral clusters. Therefore, their structure was analyzed using the data supplied by the authors [26]. One of the clusters reveals a near ideal r-PIC structure with nice tetrahedron of dh chains but with only one icosahedral unit, because the chains are too long to be closed at each end with ic units inside the cluster. However, three remaining places at the dh chain crossings can be completed by ic units if covered by one or two additional atomic layers. One of the two remaining clusters also resembles the r-PIC cluster with completed one triangle from dh chains and one ic unit, while the second one is similar to the s-IC clusters.

Experimental data on the structure of the rare-gas clusters of the size $N<1000$, as in this work, are sparse in the recent literature of the last decade. The published results [4,27,28] are very interesting though they are not still very precise regarding the structure determination, mainly due to an unavoidable wide spectrum of structures and cluster sizes. The report of Kakar *et al.* [4] for the occurrence of fcc structure at $N \approx 200$ can be interpreted as detection of the first defected crystalline clusters observed in this work at $N=201$ (see Fig. 4). Analyzing the photoemission spectra of neon clusters produced by supersonic expansion, Joshi *et al.* [27] reported very recently that the fcc-structured clusters, together with smaller icosahedral clusters, may be present in the size range $40 \leqslant N \leqslant 550$ (or even ~750). This may be interpreted in terms of the existence of fcc layers or fcc tetrahedral core in defected crystalline clusters. It would also be interesting to prove the existence of the amorphous (polyicosahedral) phase in Ar clusters composed of 600–800 atoms, as deduced by Danylchenko *et al.* [28] from their electron-diffraction study. The present simulation results indicate that they could be interpreted by the presence of regular polyicosahedral clusters.

Finally, it should be mentioned that the analysis of the internal structure in large metal clusters [29–31] may be helpful in comparison with the simulated data, though different interactions are involved. The polydecahedral structure found very recently in simulated gold clusters [29] has some similarities (dh chains crossing near the surface and the angles between chains) to the r-PIC structure. The important difference, however, lies in the lack of local ic units [32]. The layered and defected layered fcc-hcp clusters were reported for simulated freezing of gold nanoparticles [30] at $N=1157$, while probably defected crystalline structures were found in copper clusters [31].

In conclusion, the transition from the noncrystalline to crystalline LJ clusters is observed to be initiated significantly at $N=309$ in agreement with the transition size $N=280$ predicted here from energy analysis. The recently reported transition sizes $N=450$ in Ref. [11] and, especially, $N=300$ in Ref. [10] are in good agreement with our results. However, the regular polyicosahedral clusters are inherently present at large sizes, in nearly equal amount, together with the defective crystalline ones. This feature is attributed to kinetic effects visible during cluster solidification initiated by an icosahedral unit on the surface of the supercooled cluster.

ACKNOWLEDGMENTS

The author thanks the State Committee for Scientific Research Poland (KBN) for financial support under Grant No. 2 P03B 027 25 and Professor Keshra Sangwal for his constant interest in this work. The author is grateful to Dr. Eva Noya and Dr. Jonathan Doye for providing the files with coordinates of clusters, as well as to Dr. Giulia Rossi and Professor Riccardo Ferrando for submission of cluster data and useful discussion.

[1] J. Farges, M. F. de Feraudy, B. Raoult, and G. Torchet, J. Chem. Phys. **84**, 3491 (1986).
[2] J. W. Lee and G. D. Stein, J. Phys. Chem. **91**, 2450 (1987).
[3] S. I. Kovalenko, D. D. Solnyshkin, E. T. Verkhovtseva, and V. V. Eremenko, Chem. Phys. Lett. **250**, 309 (1996).
[4] S. Kakar, O. Björneholm, J. Weigelt, A. R. B. de Castro, L. Tröger, R. Frahm, T. Möller, A. Knop, and E. Rühl, Phys. Rev. Lett. **78**, 1675 (1997).
[5] B. Raoult, J. Farges, M.-F. de Feraudy, and G. Torchet, Philos. Mag. B **60**, 881 (1989).
[6] J. P. K. Doye and F. Calvo, Phys. Rev. Lett. **86**, 3570 (2001).
[7] N. V. Krainyukova, Thin Solid Films **515**, 1658 (2006).
[8] B. W. van de Waal, G. Torchet, and M.-F. de Feraudy, Chem. Phys. Lett. **331**, 57 (2000).
[9] F. Baletto and R. Ferrando, Rev. Mod. Phys. **77**, 371 (2005).
[10] A. Ghazali and J.-C. S. Lévy, Phys. Lett. A **228**, 291 (1997).
[11] T. Ikeshoji, G. Torchet, M.-F. de Feraudy, and K. Koga, Phys. Rev. E **63**, 031101 (2001).
[12] W. Polak, Eur. Phys. J. D **40**, 231 (2006).
[13] W. Polak and A. Patrykiejew, Phys. Rev. B **67**, 115402 (2003).
[14] B. W. van de Waal, *The fcc/hcp Dilemma* (Febodruk BV, Enschede, 1997), Chap. 2.
[15] T. Ikeshoji, B. Hafskjold, Y. Hashi, and Y. Kawazoe, J. Chem. Phys. **105**, 5126 (1996).
[16] W. Polak, Phys. Rev. B **71**, 235413 (2005).
[17] J. Farges, M. F. de Feraudy, B. Raoult, and G. Torchet, J. Chem. Phys. **78**, 5067 (1983).
[18] W. Polak, Cryst. Res. Technol. **42**, 1207 (2007).
[19] D. J. Wales, J. P. K. Doye, A. Dullweber, M. P. Hodges, F. Y. Naumkin, F. Calvo, J. Hernández-Rojas, and T. F. Middleton, the Cambridge Cluster Database, http://www-wales.ch.cam.ac.uk./CCD.html
[20] J. A. Northby, J. Chem. Phys. **87**, 6166 (1987).
[21] D. Romero, C. Barrón, and S. Gómez, Comput. Phys. Commun. **123**, 87 (1999).
[22] X. G. Shao, Y. H. Xiang, and W. S. Cai, Chem. Phys. **305**, 69 (2004).
[23] Y. H. Xiang, L. Cheng, W. Cai, and X. G. Shao, J. Phys. Chem. A **108**, 9516 (2004).
[24] W. Polak, *Internal Structure of Liquid Lennard-Jones Clusters* (unpublished).
[25] E. G. Noya and J. P. K. Doye, J. Chem. Phys. **124**, 104503 (2006).
[26] E. G. Noya and J. P. K. Doye (private communication).
[27] S. Joshi, S. Barth, S. Marburger, V. Ulrich, and U. Hergenhahn, Phys. Rev. B **73**, 235404 (2006).
[28] O. G. Danylchenko, S. I. Kovalenko, and V. N. Samovarov, Low Temp. Phys. **30**, 743 (2004).
[29] G. Rossi and R. Ferrando, Nanotechnology **18**, 225706 (2007).
[30] Y. Chushak and L. S. Bartell, Eur. Phys. J. D **16**, 43 (2001).
[31] S. Valkealahti and M. Manninen, J. Phys.: Condens. Matter **9**, 4041 (1997).
[32] G. Rossi and R. Ferrando (private communication).